HHS Public Access

Author manuscript

Int J Radiat Oncol Biol Phys. Author manuscript; available in PMC 2021 December 01.

Published in final edited form as:

Int J Radiat Oncol Biol Phys. 2020 December 01; 108(5): 1240–1247. doi:10.1016/j.ijrobp.2020.06.071.

A Multi-atlas Approach for Active Bone Marrow Sparing Radiation Therapy: Implementation in the NRG-GY006 Trial

Tahir Yusufaly, PhD[#*], **Austin Miller, PhD**[†], **Ana Medina-Palomo, PhD**[#*], **Casey W. Williamson, MD**[*], **Hannah Nguyen, MS, CMD**[‡], **Jessica Lowenstein, MD**[‡], **Charles A. Leath III, MD**[§], **Ying Xiao, PhD**[‖], **Kevin L. Moore, PhD**[*], **Katherine M. Moxley, MD**[¶], **Carlos M. Chevere-Mourino, MD**[#], **Tony Y. Eng, MD**[**], **Tarrick Zaid, MD**[††], **Loren K. Mell, MD**[*]

[*]Department of Radiation Medicine and Applied Sciences, University of California San Diego, La Jolla, California

[†]NRG Oncology, Statistics and Data Management Center, Roswell Park Cancer Institute, Buffalo, New York

[‡]IROC Houston QA Center, MD Anderson, Houston, Texas

[§]Department of Gynecologic Oncology, University of Alabama Birmingham, Birmingham, Alabama

[‖]Department of Medical Physics, University of Pennsylvania, Philadelphia, Pennsylvania

[¶]Stephenson Cancer Center, University of Oklahoma, Oklahoma City, Oklahoma

[#]Radiation Oncology Center, Comprehensive Cancer Center, University of Puerto Rico, San Juan, Puerto Rico

[**]Department of Radiation Oncology, Winship Cancer Institute of Emory University, Atlanta, Georgia

[††]TA Methodist Hospital System, Houston Methodist Hospital, Houston, Texas

[#] These authors contributed equally to this work.

Abstract

Purpose: Sparing active bone marrow (ABM) can reduce acute hematologic toxicity in patients undergoing chemoradiotherapy for cervical cancer, but ABM segmentation based on positron emission tomography/computed tomography (PET/CT) is costly. We sought to develop an atlas-based ABM segmentation method for implementation in a prospective clinical trial.

Methods and Materials: A multiatlas was built on a training set of 144 patients and validated in 32 patients from the NRG-GY006 clinical trial. ABM for individual patients was defined as the subvolume of pelvic bone greater than the individual mean standardized uptake value on registered ^{18}F-fluorodeoxyglucose PET/CT images. Atlas-based and custom ABM segmentations were compared using the Dice similarity coefficient and mean distance to agreement and used to

Corresponding author: Loren K. Mell, MD; lmell@health.ucsd.edu.

Research data are not available at this time.

Supplementary material for this article can be found at https://doi.org/10.1016/j.ijrobp.2020.06.071.

generate ABM-sparing intensity modulated radiation therapy plans. Dose-volume metrics and normal tissue complication probabilities of the two approaches were compared using linear regression.

Results: Atlas-based ABM volumes (mean [standard deviation], 548.4 [88.3] cm^3) were slightly larger than custom ABM volumes (535.1 [93.2] cm^3), with a Dice similarity coefficient of 0.73. Total pelvic bone marrow V_{20} and D_{mean} were systematically higher and custom ABM V_{10} was systematically lower with custom-based plans (slope: 1.021 [95% confidence interval (CI), 1.005-1.037], 1.014 [95% CI, 1.006-1.022], and 0.98 [95% CI, 0.97-0.99], respectively). We found no significant differences between atlas-based and custom-based plans in bowel, rectum, bladder, femoral heads, or target dose-volume metrics.

Conclusions: Atlas-based ABM segmentation can reduce pelvic bone marrow dose while achieving comparable target and other normal tissue dosimetry. This approach may allow ABM sparing in settings where PET/CT is unavailable.

Introduction

Hematologic toxicity is a significant clinical problem for patients with cervical cancer treated with concurrent chemoradiotherapy.[1] Numerous studies indicate that increased pelvic bone marrow (PBM) radiation dose, particularly to subregions with high cellularity, metabolic activity, and/or proliferation, is associated with increased toxicity and poorer tolerance to chemotherapy.[2–8]

As a strategy to avoid “active” bone marrow (ABM), image guided intensity modulated radiation therapy (IG-IMRT) has been implemented with the aid of functional imaging, such as ^{18}F-fluorodeoxyglucose (FDG) or ^{18}F-fluorothymidine positron emission tomography/computed tomography (PET/CT).[6,8–10] ABM sparing has advantages over whole-PBM sparing, because the latter can unnecessarily constrain planning optimization, compromising target coverage or other organs at risk (OARs). However, functional imaging techniques are expensive and commonly unavailable in resource-constrained settings.

To address this problem, previous authors proposed methods to predict the location of ABM regions using spatial statistical models or atlases based on deformable image registration, potentially obviating the need for expensive functional imaging to create “custom” ABM-sparing plans.[11,12] This approach assumes that ABM distributions follow relatively predictable, canonical patterns within the PBM space. Although these studies demonstrated proof-of-principle in single institution academic settings, implementing atlas-based ABM sparing in a multicenter setting requires separate validation studies to ensure clinical feasibility in the general cervical cancer population.

In this study, we test the feasibility and reliability of a cross-platform approach to atlas-based ABM segmentation for application in a multi-institutional trial, NRG-GY006.[13] This trial offers a large and diverse data set with which to validate and clinically implement atlas-based ABM segmentation. We applied established knowledge-based planning protocols,[14] optimized for ABM sparing, to provide real-time feedback quality control to clinics to

maximize normal tissue sparing. Simultaneously, we compared atlas-based versus custom ABM segmentation, to determine the effect on target coverage and OAR sparing.

Methods and Materials

Sampling methods

The NRG-GY006 trial is investigating standard chemoradiotherapy with or without concurrent triapine for patients with locoregionally advanced cervical cancer. The initial study design was a phase II randomized trial. After the first 189 patients were enrolled, the study was expanded to a phase III trial, with a planned sample size of 450 patients. The phase III trial is currently enrolling.

All institutions participating in this trial undergo central review and credentialing for both FDG-PET/CT and 3D conformal radiation therapy plan quality assurance. Optionally, sites can also apply for IG-IMRT credentialing through a separate process. All patients undergo a pretreatment FDG-PET/CT and receive either 3D conformal radiation therapy or IG-IMRT. Once sites are credentialed for IG-IMRT, all newly enrolled patients at that institution must be treated with IG-IMRT. The IG-IMRT technique used in phase II patients involved customized ABM sparing using segmentation based on the pretreatment FDG-PET/CT, while the IG-IMRT technique used in phase III patients involved the atlas-based ABM-sparing technique described in later sections.

Training set selection and atlas construction

The initial training sample for the atlas consisted of 189 patients enrolled in the phase II portion of NRG-GY006. Of these 189, 45 patients were excluded due to ineligibility, withdrawal, lack of imaging data, or poor image quality, resulting in a 144-patient training set (Fig. 1).

Target volumes and OARs, including PBM, were contoured on the planning CT provided by each institution. The PBM was contoured as a solid continuous structure, including the os coxae, L4 and L5 vertebral bodies, sacrum, acetabula, and proximal femora to the level of the ischial tuberosities, and excluding the spinal canal. To generate the custom ABM (gold standard) for each subject, first the PET/CT scan was deformably registered to the simulation CT and the PBM volume was transferred to the PET/CT scan. The mean body weight-corrected standardized uptake value (SUV) was quantified within total bone, and ABM was identified as subregion with an SUV greater than the individual patient’s mean SUV within the total bone, as previously described.[8] Finally, this newly derived ABM volume was transferred back to the planning CT.

It is worth briefly commenting on the choice of ABM definition. Specifically, one might ask why we do not use a predetermined SUV threshold, as opposed to thresholds standardized to individual patients. The latter method has a stronger rationale, due to less dependence on interscan and platform variation and less variation with respect to age-related changes in the marrow. To arrive at a clinically meaningful subregion to avoid in treatment planning, the ABM volume also has to be not too large and not too small relative to the surrounding bone structure. It should be noted that regions of activity so defined for a given patient might not

be considered active compared with the general population, but it makes sense physiologically to spare regions that are relatively more active in the given patient, rather than compared with a population mean. Moreover, this is the approach that has been adopted in prospective clinical trials, with associated observed reductions in hematologic toxicity and improved chemotherapy tolerance. Although the method will likely exclude some active areas and include some inactive areas of the marrow, this is in exchange for identifying a canonical avoidance structure that is clinically applicable for each patient, independent of PET availability and less prone to outliers.

After generating the custom ABMs for the training set, 1 patient with an average height and weight and an intermediate-sized PBM volume (1223.91cc) was selected to serve as the template. The remaining 143 patients, along with their custom ABM contours, were added to the atlas, using the platform directly built into the MIM Maestro software.[15]

Atlas validation

To validate the atlas, 32 patients enrolled during late phase II (n = 9) or at the onset of phase III (n = 3), along with “dry run” cases submitted during the credentialing phase (n = 20), comprised the test sample. The latter set, consisting of imaging data from previously treated patients with cervical cancer submitted by the institution undergoing credentialing, was included to try to assess a more general “off-protocol” application of the ABM atlas. Automatic atlas-based ABM contours were generated using the atlas constructed in the MIM Maestro platform during the training phase. The atlas segmentation algorithm in MIM works via a multiatlas approach, using a majority vote inclusion criterion.[16] For each new patient, the algorithm searches the 144-patient atlas database to find the 5 to 6 best-matching patients, as quantified by Dice similarity coefficient (DSC) of the pelvic CT body contours, and then deformably registers those best matches to the new patient using the default algorithm in MIM, a free-form, intensity-based approach using the entire CT contrast window. Each voxel is then examined to see how many times it is labeled as ABM based on the best matches, and if a voxel is labeled ABM in at least 3 of the matches, it is included in the atlas-based ABM segmentation. Of the 9 phase II test patients, 8 were also included in the final atlas database; however, these were excluded from the atlas during testing, by allowing the algorithm to search only the other 143 patients.

Subsequently, we compared atlas-based ABM with the custom ABM using the DSC and mean distance of agreement (MDA). To compare atlas-based ABM-sparing versus custom ABM-sparing IG-IMRT plans, 2 plans were generated for each patient, using the RapidPlan KBP software (Varian, Palo Alto, CA). Plans were optimized for coverage of the planning target volume (PTV) and sparing of 6 OARs: PBM, femoral heads, bowel, bladder, rectum, and either the atlas-based (for the first plan) or custom (for the second plan) ABM structure. The clinical target volume consisted of the gross tumor, parametria, upper vagina, and pelvic lymph nodes, with an anisotropic planning margin of 0.5-1.5 cm to create the PTV. For patients with gross pelvic nodal involvement, PTV_{boost} was defined as a 5 mm expansion around the involved node. All plans were generated using the Eclipse treatment planning system (Varian) and prescribed as either 45.0 Gy in 1.8 Gy daily fractions (n = 23), or 47.60 Gy in 28 fractions with a simultaneous integrated boost of 54.0-59.4 Gy to PTV_{boost} (n = 9).

Paired *t* tests were used to test the null hypothesis of no difference between atlas-based and custom ABM contours in terms of DSC and MDA, with *P* values < .05 considered statistically significant and Bonferroni corrections applied to account for multiple hypothesis testing. Mean dose-volume metrics and averaged dose-volume histograms were also calculated and compared between the 2 plans, using linear regression to relate atlas-based metrics to custom-based metrics, with the precise fitting being custom plan value = slope*(atlas plan value) + error.

Results

Demographic features for the training and test samples are shown in Table 1. A total of 168 subjects were analyzed: 136 trial subjects were in the training set only, 4 trial subjects were in the test set only, 8 trial subjects were in both the training and test set (with data removed from the training set during testing), and 20 credentialing subjects were in the test set only. Demographic data for the 20 credentialing subjects were unavailable. Individual-level data for trial patients were also unavailable, because the trial is ongoing.

The mean (standard deviation [SD]) ABM and PBM volumes for patients in the training set were 551.6 (88.6) cc and 1237.5 (182.1) cc, respectively, corresponding to an ABM/PBM ratio of 44.6% (2.49%). The median (interquartile range) ABM volume, PBM volume, and ratio were 540.6 (487.5-610.9) cm^3, 1215.5 (1098.7-1364.6) cm^3, and 44.5% (42.9-46.1%), respectively. In the test set, the mean (SD) custom ABM, atlas ABM, and PBM volumes were 535.1 (93.2) cm^3, 548.4 (88.3) cm^3, and 1191.9 (189.6) cm^3, respectively, corresponding to a custom ABM/PBM ratio of 44.8% and atlas ABM/PBM ratio of 46.1%.

Although the difference in custom versus atlas ABM volumes was statistically significant (*P* = .015), the mean (SD) DSC and MDA for custom and atlas-based ABM were 0.73 (0.06) and 2.51 mm (0.83 mm), respectively, indicating overall good agreement between both volumes despite the difference in absolute volumes. Figure 2 juxtaposes a canonical individualized distribution of ABM within pelvic bone versus ABM rendered using the atlas, depicting good agreement as well.

Dosimetric comparisons of custom versus atlas ABM-sparing plans are shown in Table 2 and Figure 3. Overall, we observed no significant differences between atlas-based and custom-based ABM-sparing IMRT plans in any dose-volume metrics (bowel, rectum, bladder, femoral heads, ABM, or target volumes), with the exception of PBM, which had consistently *lower* V_{20} and D_{mean} with atlas-based plans, and custom ABM, which had consistently higher V_{10} with atlas-based plans. More explicitly, PBM V_{20} and D_{mean} were systematically higher and custom ABM V_{10} was systematically lower with custom-based plans (slope: 1.021 [95% confidence interval (CI), 1.005-1.037], 1.014 [95% CI, 1.006-1.022], and 0.98 [95% CI, 0.97-0.99], respectively). For ABM, dose-volume histogram comparisons between custom- and atlas-based ABM-sparing IG-IMRT plans, as highlighted in Figure 3, indicated no significant dosimetric gains using individualized PET/CT-guided plans compared with the atlas. Moreover, despite statistical differences between custom versus atlas ABM volumes, these did not translate into clinically significant differences in mean dose for the custom ABM (Fig. E1).

Discussion

In this study, we found that an atlas based on a multi-institutional cohort of 144 patients enrolled in the NRG-GY006 trial was effective in predicting the location of pelvic bone marrow subregions with high metabolic activity as defined by FDG-PET/CT. Furthermore, plans designed to spare atlas-based ABM performed comparably to customized planning, indicating that this approach could obviate the need for individual functional imaging for the purpose of ABM-sparing radiation therapy. This could help facilitate such a planning strategy in resource-constrained settings. Collectively, our results provide the first prospective evidence that IMRT planning using atlas-based ABM segmentation is a feasible bone marrow sparing approach in the multi-institutional setting. Furthermore, many institutions have no way of determining ABM, so an atlas-based approach that spares the most likely locations of ABM would presumably be better than a plan with no ABM contour at all.

Interestingly, we found that ABM-sparing IMRT plans based on the atlas were as effective in sparing the *custom* ABM (as measured by the V_{20} and D_{mean}) as the IMRT plans based directly on custom ABM itself. This rather counterintuitive finding was observed in a previous study as well[16] and may be due to atlas-based ABM segmentation being more robust to outliers than custom ABM segmentation, as demonstrated in Figure 4. Furthermore, atlas-based ABM-sparing IMRT plans achieved a slightly lower overall dose to PBM, which also has been previously observed.[16] No dosimetric differences between custom- and atlas-based plans were observed for the remaining OARs or targets. In particular, the atlas-based plans did not appear to compromise target coverage or bowel sparing, as was observed in a previous study.[12] We suspect this is a consequence of the atlas segmentation algorithm using multiatlas matching with majority vote selection, whereas the previous work used a single averaged atlas as a template, limiting its ability to capture patient diversity and variability.

Although this study overall demonstrates the feasibility of clinical implementation of an atlas-based approach to ABM-sparing radiation therapy, there are still further directions to be explored. In particular, phase III of the NRG-GY006 trial is currently assessing effects on hematologic toxicity by directly using the atlas-based ABM contours instead of custom-based ABM contours, in clinical real time. Additionally, although previous experience strongly suggests that ABM sparing is causally related to reduction in hematologic toxicity, more outcomes data are required to conclusively verify that an atlas-based approach to ABM sparing directly improves patient outcomes.

The main strength of this study lies in the size and diversity used to generate the multiatlas database, as well as its availability and accessibility — it can be exported and used by any institution with access to MIM software. We note that the atlas in its current form is limited to the MIM platform; however, the methodology can in principle be generalized to other software platforms, as the essential algorithm is not MIM-dependent. Further work is ongoing to develop a platform-independent atlas for clinical applications. The atlas can be extended to include more patients, although users must note that this comes with an increase in computational time that may not provide sufficient new relevant information to justify the

costs. It is also worth mentioning that although we have focused on the ABM, the segmentation atlas can also generate PBM structures used for the generation of IMRT plans faster than manual contouring, with the possibility for manual correction of atlas-generated PBM structures.

Supplementary Material

Refer to Web version on PubMed Central for supplementary material.

Acknowledgments—

The following Gynecologic Oncology Group member institutions participated in the primary treatment studies: University of Oklahoma, San Juan City Hospital, University of California at San Diego, Emory University – Winship, TA Methodist Hospital System, Riverside Methodist Hospital, UAMS, Augusta University Medical Center, Lewis Cancer and Research Pavilion, Northwestern University, UMC New Orleans, East Jefferson Hospital, Radiation Oncology Centers of Nevada, Mount Sinai Chelsea, Cleveland Clinic Foundation, Case Western Reserve University, University of Cincinnati, CR Spartanburg Medical Center, Greenville Health System, UT Southwest Medical Center, TA Froedtert and Medical College of Wisconsin, Aurora West Allis Medical Center, West Virginia University, University of Health - James Graham Brown Cancer Center, and Lewis Cancer & Research Pavilion.

This work was supported by National Cancer Institute (NCI) grants to Dr Mell and Dr Moore (1R01CA197059-01), NRG Oncology (U10 CA180822), NRG Operations (U10 CA180868), NCI Community Oncology Research Program (NCORP) (UG1CA189867), and Imaging and Radiation Oncology Core (IROC) (U24CA180803).

Disclosures: C.A.L. reports grants from NIH during the conduct of the study and K.L.M. reports grants, personal fees, and nonfinancial support from Varian Medical Systems outside the submitted work.

References

1. Torres MA, Jhingran A, Thames HD, et al. Comparison of treatment tolerance and outcomes in patients with cervical cancer treated with concurrent chemoradiotherapy in a prospective randomized trial or with standard treatment. Int J Radiat Oncol Biol Phys 2008;70:118–125. [PubMed: 17869451]
2. Mell LK, Kochanski JD, Roeske JC, et al. Dosimetric predictors of acute hematologic toxicity in cervical cancer patients treated with concurrent cisplatin and intensity-modulated pelvic radiotherapy. Int J Radiat Oncol Biol Phys 2006;66:1356–1365. [PubMed: 16757127]
3. Rose BS, Aydogan B, Liang Y, et al. Normal tissue complication probability modeling of acute hematologic toxicity in cervical cancer patients treated with chemoradiotherapy. Int J Radiat Oncol Biol Phys 2011;79:800–807. [PubMed: 20400238]
4. Yang Y, Li W, Qian J, Zhang J, Shen Y, Tian Y. Dosimetric predictors of acute hematologic toxicity due to intensity-modulated pelvic radiotherapy with concurrent chemotherapy for pelvic cancer patients. Transl Cancer Res 2018;7:515–523.
5. Albuquerque K, Giangreco D, Morrison C, et al. Radiation-related predictors of hematologic toxicity after concurrent chemoradiation for cervical cancer and implications for bone marrow–sparing pelvic IMRT Int J Radiat Oncol 2011;79:1043–1047.
6. Rose BS, Liang Y, Lau SK, et al. Correlation between radiation dose to ^{18}F-FDG-PET defined active bone marrow subregions and acute hematologic toxicity in cervical cancer patients treated with chemoradiotherapy. Int J Radiat Oncol Biol Phys 2012;83:1185–1191. [PubMed: 22270171]
7. Klopp AH, Moughan J, Portelance L, et al. Hematologic toxicity in RTOG 0418: A phase 2 study of postoperative IMRT for gynecologic cancer. Int J Radiat Oncol Biol Phys 2013;86:83–90. [PubMed: 23582248]
8. Mell LK, Siráak I, Wei L, et al. Bone marrow-sparing intensity modulated radiation therapy with concurrent cisplatin for stage IB-IVA cervical cancer: An international multicenter phase II clinical trial (INTERTECC-2). Int J Radiat Oncol Biol Phys 2017;97:536–545. [PubMed: 28126303]

9. Elicin O, Callaway S, Prior JO, Bourhis J, Ozsahin M, Herrera FG. [(18)F]FDG-PET standard uptake value as a metabolic predictor of bone marrow response to radiation: Impact on acute and late hematological toxicity in cervical cancer patients treated with chemoradiation therapy. Int J Radiat Oncol Biol Phys 2014;90:1099–1107. [PubMed: 25442041]
10. Wyss JC, Carmona R, Karunamuni RA, Pritz J, Hoh CK, Mell L K. [(18)F] Fluoro-2-deoxy-2-d-glucose versus 3'-deoxy-3'-[(18)F]fluorothymidine for defining hematopoietically active pelvic bone marrow in gynecologic patients. Radiother Oncol J Eur Soc Ther Radiol Oncol 2016;118:72–78.
11. McGuire SM, Menda Y, Ponto LLB, et al. Spatial mapping of functional pelvic bone marrow using FLT PET. J Appl Clin Med Phys 2014;15:129–136. [PubMed: 25207403]
12. Li N, Noticewala SS, Williamson CW, et al. Feasibility of atlas-based active bone marrow sparing intensity modulated radiation therapy for cervical cancer. Radiother Oncol J Eur Soc Ther Radiol Oncol 2017; 123:325–330.
13. Radiation therapy and cisplatin with or without triapine in treating patients with newly diagnosed stage IB2, II, or IIIB-IVA cervical cancer or stage II-IVA vaginal cancer - Full Text View - ClinicalTrials.gov. Available at: https://clinicaltrials.gov/ct2/show/NCT02466971. Accessed November 8, 2019.
14. Li N, Carmona R, Sirak I, et al. Highly efficient training, refinement, and validation of a knowledge-based planning quality-control system for radiation therapy clinical trials. Int J Radiat Oncol 2017;97:164–172.
15. Patel R, Traughber B, Kaminsky D, et al. Evaluation of an Atlas-based segmentation method for high-risk prostate cancer with RTOG-defined pelvic lymph node levels. Int J Radiat Oncol Biol 2014;90: S74–S75.
16. Iglesias JE, Sabuncu MR. Multiatlas segmentation of biomedical images: A survey. Med Image Anal 2015;24:205–219. [PubMed: 26201875]

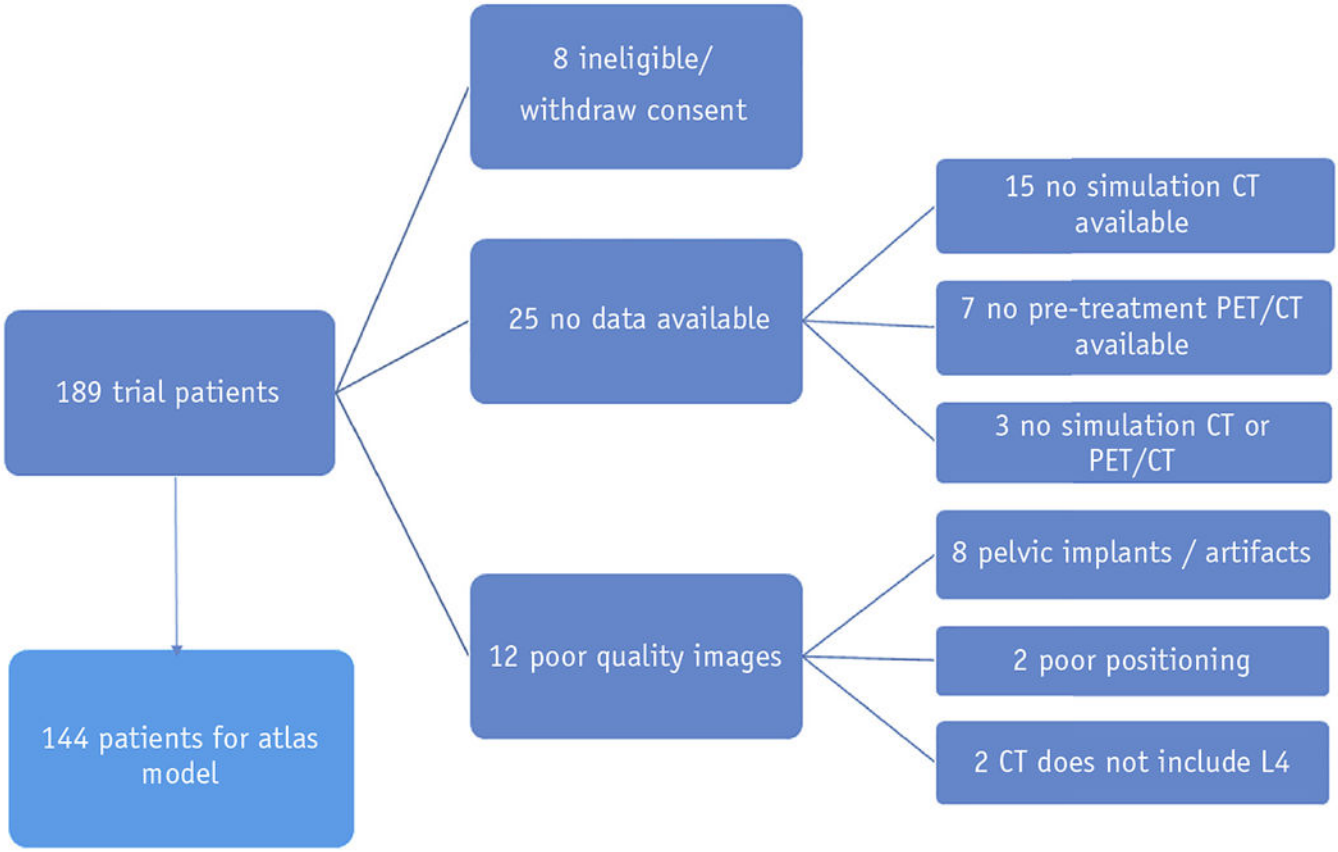

Fig. 1.

Flow diagram showing exclusion criteria applied to the training sample used to construct and validate an active bone marrow atlas. *Abbreviations:* CT = computed tomography; PET = positron emission tomography.

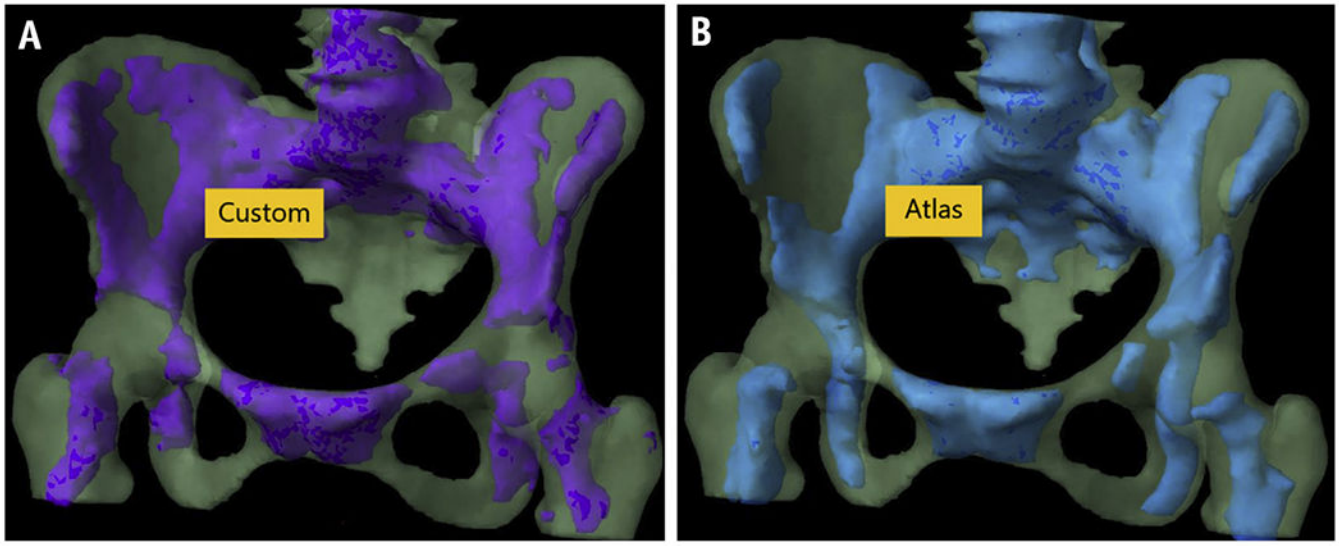

Fig. 2.

Canonical distribution of metabolically “active” bone marrow subregions in a patient with cervical cancer, with “active” marrow defined either by custom (A) positron emission tomography–based segmentation or (B) multiatlas-based segmentation.

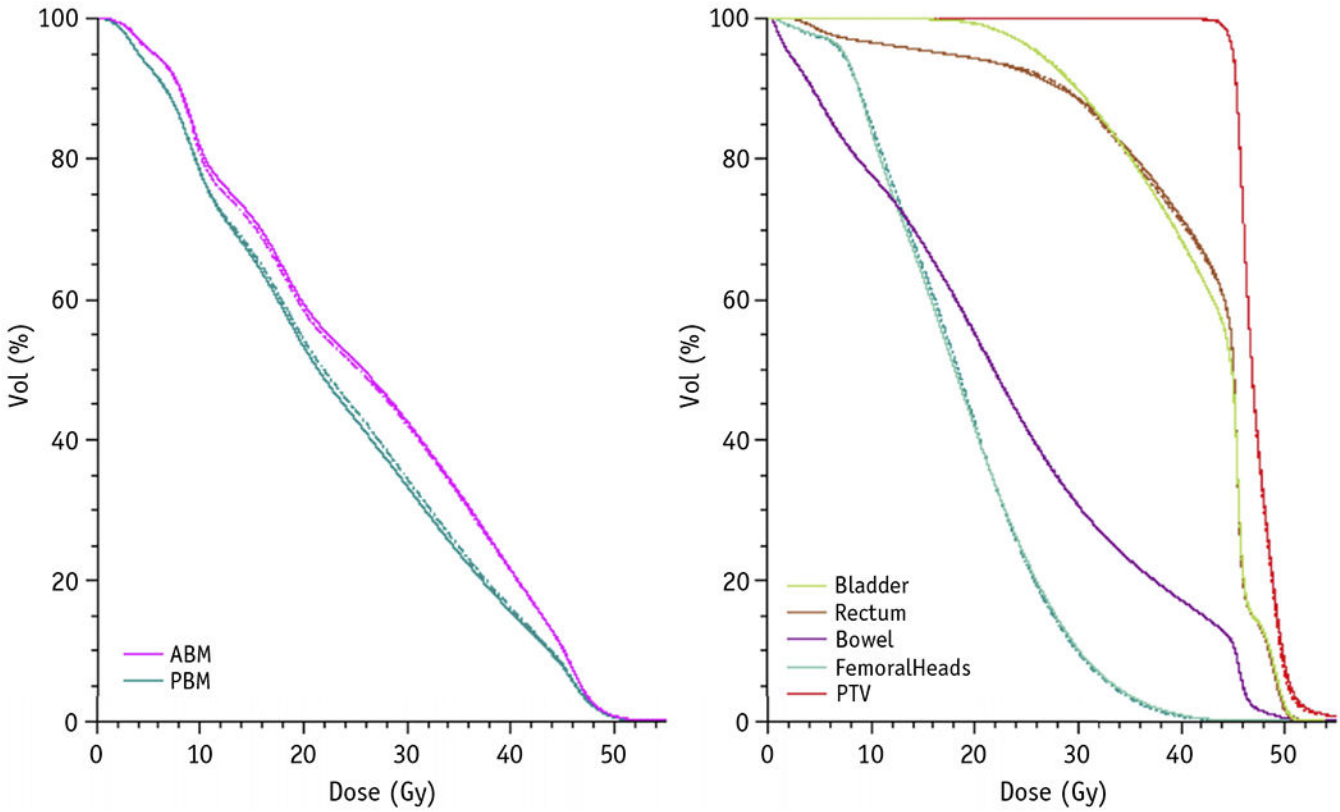

Fig. 3.

Averaged dose-volume histogram (DVH) comparison for custom plans designed to spare active bone marrow (ABM) defined by positron emission tomography (PET) (dashed lines) versus ABM-sparing plans based on the atlas (solid lines), indicating similar results using either approach. Note the DVHs for ABM (left) depict results for the ABM that is defined by PET, indicating that *atlas*-based plans, on average, result in good sparing of the *custom* ABM. *Abbreviation:* PTV = planning target volume.

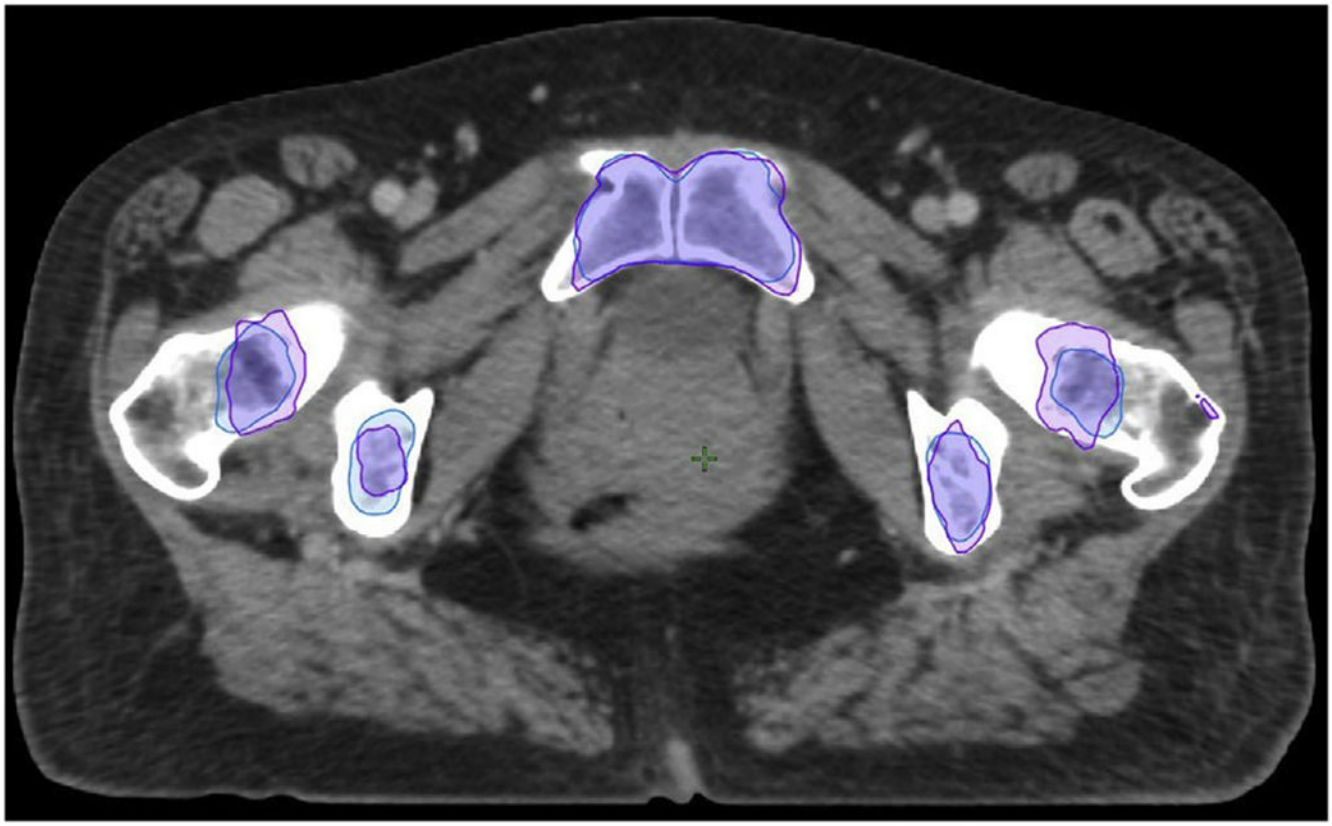

Fig. 4.

The custom-based active bone marrow (purple) may include outliers, such as seen in the left femur in this patient. The atlas-based method (blue), by virtue of averaging, removes outliers, consequently avoiding unnecessarily restrictive planning constraints that potentially compromise sparing of the overall pelvic bone volume.

Table 1

Demographic characteristics of the training and test samples

	Test set (available data) (n = 12)	Training set only (n = 136)	Total (n = 148)
Age (years)			
Median	44	46	46
Min-max	30-82	27-82	27-82
Q1 (first quartile) - Q3 (third quartile)	41.5-60.5	38-56	38-56
20-29	0 (0.0%)	5 (3.7%)	5 (3.4%)
30-39	2 (16.7%)	39 (28.7%)	41 (27.7%)
40-49	6 (50.0%)	42 (30.9%)	48 (32.4%)
50-59	1 (8.3%)	25 (18.4%)	26 (17.6%)
60-69	1 (8.3%)	17 (12.5%)	18 (12.2%)
70-79	1 (8.3%)	7 (5.1%)	8 (5.4%)
80-89	1 (8.3%)	1 (0.7%)	2 (1.4%)
Ethnicity			
Hispanic	2 (16.7%)	27 (19.9%)	29 (19.6%)
Non-Hispanic	10 (83.3%)	106 (77.9%)	116 (78.4%)
Unknown/not reported	0 (0.0%)	3 (2.2%)	3 (2.0%)
Race			
Unknown/not reported	0 (0.0%)	4 (2.9%)	4 (2.7%)
Asian	1 (8.3%)	2 (1.5%)	3 (2.0%)
Black/African American	2 (16.7%)	15 (11.0%)	17 (11.5%)
American Indian/Alaskan	0 (0.0%)	2 (1.5%)	2 (1.4%)
More than 1 race	0 (0.0%)	1 (0.7%)	1 (0.7%)
White	9 (75.0%)	112 (82.4%)	121 (81.8%)
Performance status			
0	9 (75.0%)	110 (80.9%)	119 (80.4%)
1	3 (25.0%)	26 (19.1%)	29 (19.6%)
Histology			
Adenocarcinoma, unsp.	0 (0.0%)	29 (21.3%)	29 (19.6%)
Adenosquamous	0 (0.0%)	4 (2.9%)	4 (2.7%)

	Test set (available data) (n = 12)	Training set only (n = 136)	Total (n = 148)
Squamous cell carcinoma	12 (100.0%)	103 (75.7%)	115 (77.7%)
FIGO stage			
I	1 (8.3%)	28 (20.6%)	29 (19.6%)
II	7 (58.3%)	77 (56.6%)	84 (56.8%)
III	3 (25.0%)	23 (16.9%)	26 (17.6%)
IV	1 (8.3%)	8 (5.9%)	9 (6.1%)
Site of disease			
Cervix	11 (91.7%)	128 (94.1%)	139 (93.9%)
Vagina	1 (8.3%)	8 (5.9%)	9 (6.1%)
Planned brachytherapy			
HDR	12 (100.0%)	132 (97.1%)	144 (97.3%)
LDR	0 (0.0%)	4 (2.9%)	4 (2.7%)
Planned IG-IMRT			
No	0 (0.0%)	33 (24.3%)	33 (22.3%)
Yes	12 (100.0%)	103 (75.7%)	115 (77.7%)
Randomized treatment			
RT + CIS	4 (33.3%)	70 (51.5%)	74 (50.0%)
RT + CIS + 3AP	8 (66.7%)	66 (48.5%)	74 (50.0%)

Abbreviations: 3AP = Triapine; CIS = cisplatin; FIGO = International Federation of Gynecology and Obstetrics; HDR = high-dose-rate; IG-IMRT = image guided intensity modulated radiation therapy; LDR = low dose rate; RT = radiation therapy.

Table 2

Regression results testing the consistency between atlas-based plans and custom-based plans for various dose metrics

	Slope estimate	95% confidence interval
PBM		
V_{10}, %	1.004	[0.995-1.012]
V_{20}, %	1.021	[1.005-1.037]
D_{mean}, Gy	1.014	[1.006-1.022]
ABM_{custom}		
V_{10}, %	0.982	[0.972-0.993]
V_{20}, %	0.997	[0.976-1.020]
D_{mean}, Gy	1.006	[0.991-1.020]
Bowel		
D_{30}, Gy	1.003	[0.992-1.013]
D_{max}, Gy	0.998	[0.995-1.001]
V_{45}, cc	0.998	[0.985-1.011]
Rectum		
D_{50}, Gy	0.999	[0.997-1.002]
D_{60}, Gy	0.999	[0.996-1.003]
$^{D}max^{,\,Gy}$	0.996	[0.992-1.000]
Bladder		
D_{50}, Gy	0.998	[0.996-1.000]
D_{max}, Gy	0.999	[0.994-1.003]
Femoral heads		
D_{15}, Gy	0.986	[0.946-1.025]
D_{max}, Gy	0.84 (0.07) 0.994	[0.980-1.019]
PTV_{45} (n = 23)		
D_{95}, Gy	1.000	[0.999-1.000]
D_{97}, Gy	1.000	[0.999-1.001]
D_{99}, Gy	1.001	[0.999-1.003]
D_{95}, Gy	1.002	[0.999-1.004]
$PTV_{47.6}$ (n = 9)		
(n = 9)		
D_{97}, Gy	1.003	[0.999-1.006]
D_{99}, Gy	1.006	[0.999-1.013]
PTV_{Boost} (n = 9)		
D_{95}, Gy	0.999	[0.997-1.001]
D_{97}, Gy	0.999	[0.997-1.001]
D_{99}, Gy	0.999	[0.996-1.001]

Abbreviations: ABM = active bone marrow; PBM = pelvic bone marrow; PTV = planning target volume.

Each row lists the estimates and 95% confidence intervals for the best-fit slope. A slope greater than unity indicates a higher dose-volume metric for the custom-based plan relative to the atlas-based plan.